PAPER

Check for updates

Design and synthesis of versatile ligand precursors based on phosphonium ylides for palladalactam formation and catalytic investigation†

Cheng-Po Kao, Jhen-Yi Lee, Min-Cheng Tang and Hon Man Lee [iD] *

A new series of ligand precursors designed for the synthesis of palladalactams has been developed. These precursors are easily accessible through a one-step reaction involving 2-chloro-*N*-phenylacetamide and a wide choice of various monophosphines, offering tunable electronic and steric properties within the ligand framework. The stability of both ligand precursors and resulting palladalactams in ambient air enhances their practical applicability. A newly synthesized palladalactam, featuring an electron-donating triethylphosphine moiety on the anionic phosphonium ylide ligand scaffold exhibited promising catalytic activities in the Mizoroki–Heck coupling reaction between aryl chlorides and alkenes. Theoretical calculations further affirmed that the ligand system in the complex is the most electron-donating, forming the strongest Pd–C bond compared to other complexes with alternative phosphine moieties.

Introduction

Transition metal complexes involving phosphonium ylides have been attracting interest over several decades.[1–16] Recently, Gessner *et al.* introduced a pioneering class of palladium complexes featuring ylide-functionalized phosphine ligands known as YPhos (Fig. 1).[17–22] These ligands exhibit exceptional electron-donating properties, attributed to the additional contribution from the ylide group to the phosphorus center. They resemble N-heterocyclic carbene (NHC) ligands,[23–29] being neutral in their free states and serving as strong σ-donors and excellent Lewis bases for metals. Indeed, their donor capacity exceeds classical phosphines and even common NHC ligands.[17] Moreover, the extent of electron donation can be conveniently modulated by altering the substitution pattern at the ylidic carbon atom. Consequently, palladium complexes with YPhos have demonstrated outstanding catalytic activities in Pd-catalyzed reactions, particularly with unreactive aryl chloride substrates, surpassing those of palladium complexes with electron-donating phosphines such as XPhos and common NHC ligands (IMes, and IPr, *etc.*).[18–20]

Meanwhile, palladalactams, known for their distinctive four-membered metalacyclic ring system, have long been documented but remain exceptionally rare in the literature (Fig. 2).[30–34] In exploring palladium complexes with mesoionic

NHC ligands, we have concurrently uncovered an intriguing class of palladalactams.[33,34] The precursors of the ligand systems can be easily synthesized through a one-step reaction involving various imidazole derivatives and organic amides. Drawing inspiration from Gessner's works,[22] we propose a novel approach where the imidazole derivatives in our ligand system are substituted with diverse phosphines, leading to an unprecedented series of phosphonium chlorides (Scheme 1). Upon deprotonation with bases, these compounds will generate anionic phosphonium ylide ligands. Stabilizing these new ylides involves charge delocalization, encompassing the ylidic carbon, the amidate nitrogen, the carbonyl group, and the *N*-aryl ring. Like YPhos, the degree of electron donation in our new ligand can be modulated by the selection of different phosphine groups. We anticipate these ylides will serve as effective ligands for synthesizing innovative palladalactams (see Fig. 2).

This work details synthesizing a new series of phosphonium chlorides with diverse phosphine groups, showcasing their excellence as ligand precursors for preparing novel palladalactams. We further assess the catalytic efficiency of these new palladium complexes in the Mizoroki–Heck coupling reaction. In contrast to other coupling reactions, the Mizoroki–Heck coupling reaction typically necessitates higher temperatures (>100 °C), emphasizing the importance of a robust bonding between the palladium center and the ligand to prevent ligand dissociation.[35] While Pd complexes with NHC ligands have been widely employed,[36,37] exploring other robust palladium complexes with non-NHC ligands is a worthwhile endeavor. In many instances of Mizoroki–Heck coupling reactions catalyzed by Pd NHC complexes, a high Pd loading,

Department of Chemistry, National Changhua University of Education, Changhua, 500, Taiwan. E-mail: leehm@cc.ncue.edu.tw
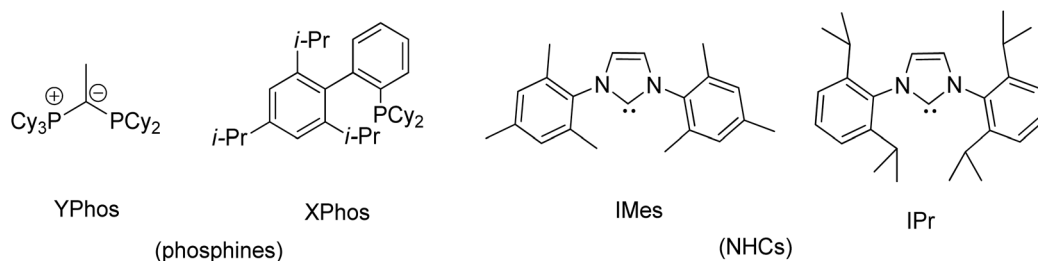
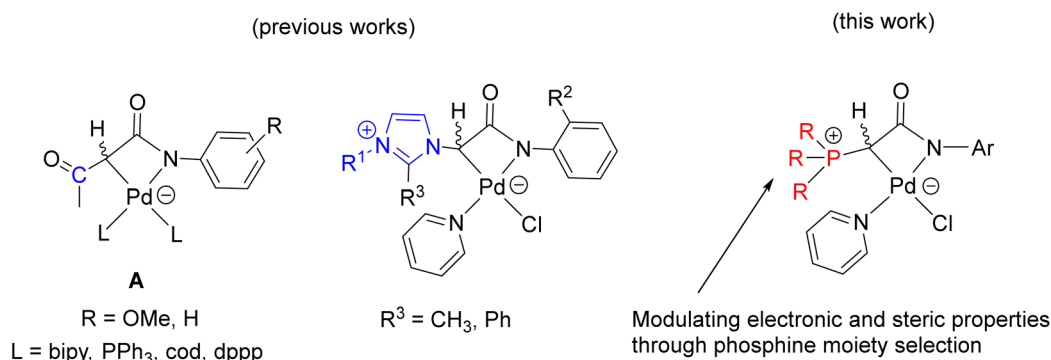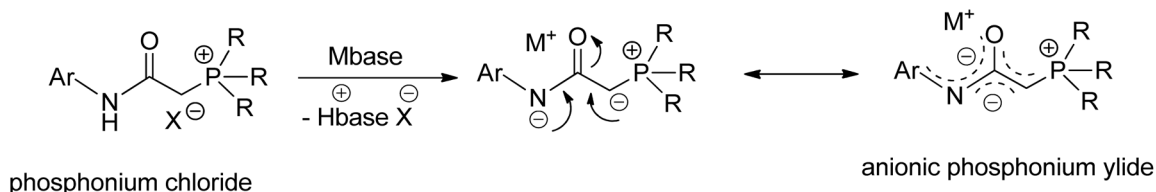**Fig. 1** Commercially available YPhos, XPhos, IPr, and IMes ligands.

Fig. 2 Palladalactams derived from functionalized acetanilide.

Scheme 1 The formation of an anionic stabilized phosphonium ylide in the presence of a base.

and more reactive and often costlier aryl bromides or iodides are typically needed as substrates.[36–45] Among our newly prepared complexes, the one containing an electron-donating trialkylphosphine moiety in the ligand system exhibited the most promising catalytic activity in the coupling of electron-deficient aryl chlorides with alkenes. Theoretical calculations revealed that the ligand system in this complex is the most electron-donating, forming the strongest Pd–C and Pd–N bonds compared to other complexes featuring alternative phosphine moieties.

## Results and discussion

Syntheses of ligand precursors and palladalactam complexes

The synthesis of ligand precursors is illustrated in Scheme 2. In a standard reaction, the ligand precursor was formed by reacting 2-chloro-N-phenylacetamide with phosphine in acetonitrile at an elevated temperature of 80 °C. Various phosphine

ligands, including trialkylphosphines and triarylphosphines, were successfully employed, resulting in good yields ranging from 76% to 84%. A salt metathesis reaction between compound **1e** and sodium tetrafluoroborate yielded the ligand precursor **1e′** with a BF$_4$ counter-anion, achieving a yield of 81%. All the ionic salt products are only sparingly soluble in common organic solvents. But they dissolve readily in highly polar solvents such as DMSO and DMF. Notably, compounds **1a** and **1d** were derived from triethylphosphine and tricyclohexylphosphine, respectively. Despite the air sensitivity of these trialkylphosphines, both compounds **1a** and **1d** exhibit stability in the presence of air after formation. The unprotected OH groups in compounds **1e** and **1e′** are well-tolerated during both synthesis and subsequent complexation reactions, likely facilitated by the formation of intramolecular OH···H hydrogen bonds, as revealed in the X-ray structures of their palladium complexes (*vide infra*).

The methylene signals of all products appear as doublets, attributed to the two-bond coupling with adjacent ^{31}P nuclei,
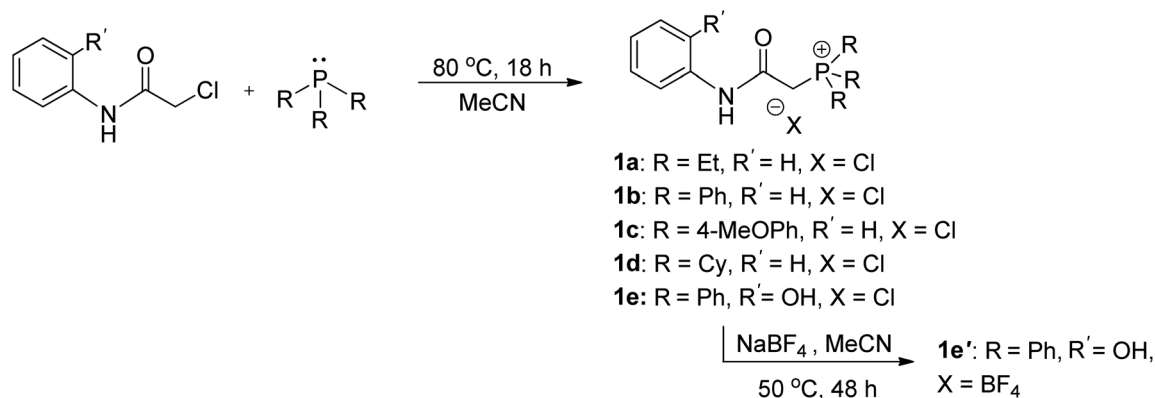
**Scheme 2** Synthesis of ligand precursors.

with a constant coupling of 15 Hz in most cases except for **1d** (12 Hz). The electron-donating nature of the phosphine moiety significantly influences the chemical shift of methylene signals. In cases involving the electron-donating trialkylphosphine moiety, a pronounced shielding effect occurs, resulting in signals resonating at an upfield chemical shift, precisely at 3.98 and 4.03 ppm in **1a** and **1d**, respectively. Conversely, compounds with triphenylphosphine moieties exhibit downfield chemical shifts above 5 ppm (**1b**, 5.43; **1c**, 5.12; **1e**, 5.32; **1e′**, 5.26 ppm). Moreover, compounds **1a** and **1d** showcase a distinct upfield shift of the α-carbon signals (**1a**, 27.2; **1d**, 23.8 ppm) compared to the others (**1b**, 32.6; **1c**, 33.3; **1e**, 32.4; **1e′**, 32.5), mirroring the trends observed in the methylene signals. These signals, appearing as doublets due to one-bond coupling with ^{31}P NMR nuclei, exhibit smaller coupling constants for electron-donating phosphine moieties (**1a**, 49.8 Hz; **1d**, 45.2 Hz) compared to those with triphenylphosphine moieties within the range of 52.8–60.3 Hz. On the contrary, the formation of phosphonium salts, resulting in formal positive charges on the phosphorus atoms, induces deshielding of the ^{31}P nuclei, leading to a downfield shift in phosphorous signals towards positive chemical shifts. Ligand precursors **1a** and **1d**, bearing electron-donating triethylphosphine and tricyclohexylphosphine, manifest more pronounced downfield shifts at 38.3 and 33.4 ppm, respectively, in contrast to those with triphenylphosphine at 21.8 ppm (**1b**, **1e**, and **1e′**). Conversely, the electron-donating 4-methoxy group on the phenyl ring causes a slightly more upfield shift of the ^{31}P NMR signal in compound **1c** compared to **1b** with a triphenylphosphine moiety (19.6 vs. 21.8 ppm). Fig. 3 shows the correlation between the ^{31}P and methylene ^{1}H NMR signal chemical shifts in the new ligand precursors.

The complexation reaction to prepare metallalactams **A** necessitated the addition of Ag$_2$O to proceed,[30,32] presumably via a transmetalation step. In contrast, in our case, direct complexation between the ligand and palladium precursors can be carried out without the need for Ag$_2$O addition. Scheme 3 illustrates the synthesis of new palladalactams using the ligand precursors. In a typical reaction, a solution of chloride salts and PdCl$_2$ in pyridine, with K$_2$CO$_3$ as a base at room
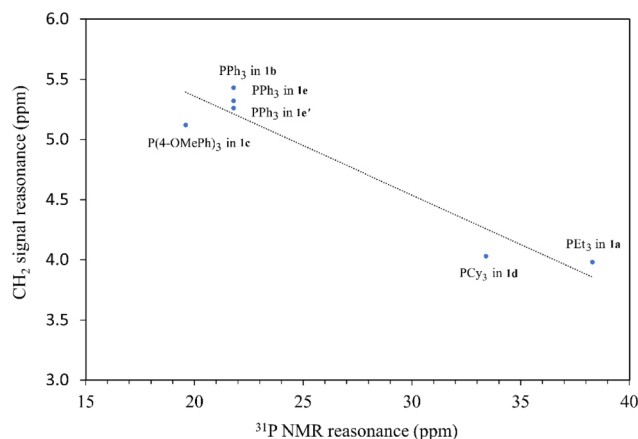
Fig. 3 The correlation between the ^{31}P and methylene ^{1}H NMR signal chemical shifts in the new ligand precursors.

temperature, leads to the formation of compounds **2a–d**. Compound **2e**, featuring a hydroxy group on the phenyl ring of the triphenylphosphine moieties, was synthesized using Pd (OAc)$_2$ and NaOAc as the base. The complexes were obtained in good yields, ranging from 54% to 74%. Confirmation of the coordination of a pyridine ligand around the palladium center in these complexes is attained through the presence of pyridine signals in their ^{1}H NMR spectra. Upon coordination, the ^{31}P NMR signals of the complexes shift downfield. The difference in chemical shifts between the complex and the ligand is more minor for those containing trialkylphosphine (Δ = 1.2 ppm for **2a** and Δ = 2.1 ppm for **2d**), whereas the shift is much more substantial (ca. 6.3 ppm) for those containing PPh$_3$ or P(4-OMePh)$_3$ moieties. Interestingly, the doublets corresponding to the coordinated CH ylide carbons in **2a** and **2d** were detected at −2.9 and −8.1 ppm, respectively, in stark contrast to all other complexes where contrasting downfield signals with positive ppm values ranging from 7.0 to 9.2 were observed. These distinctive negative ppm values in **2a** and **2d** are likely attributed to the electron-donating property of the PEt$_3$ and PCy$_3$ moieties, resulting in a higher electron density
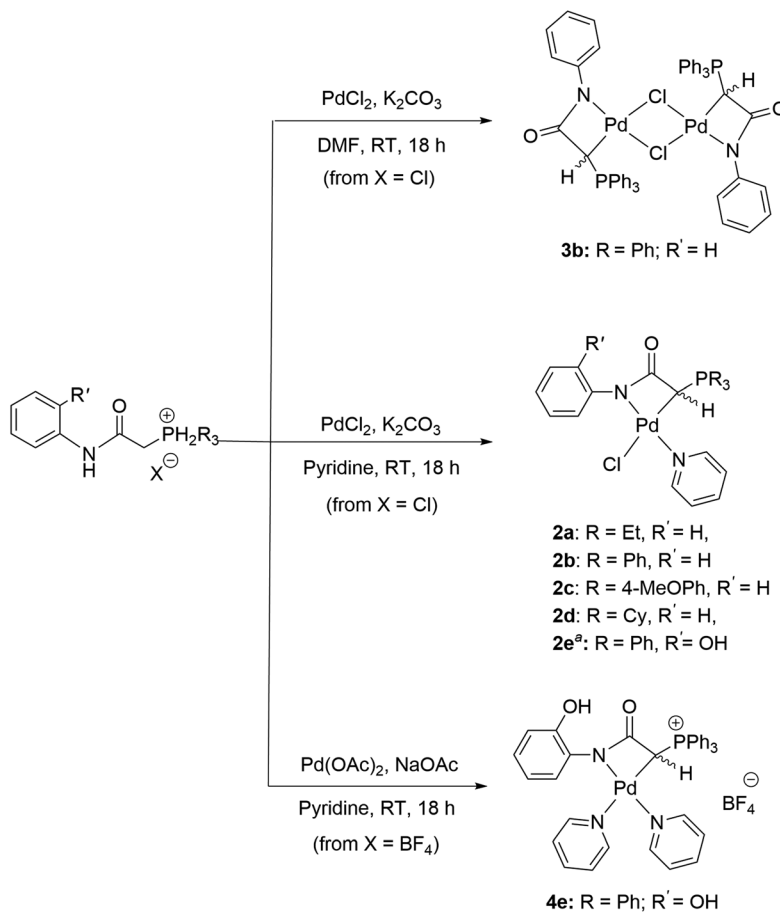
Scheme 3 Synthesis of palladalactams. [a] For the synthesis of **2e**, Pd(OAc)$_2$ and NaOAc were used.

on the carbon atom compared to ligands with PPh$_3$ moieties, thus shielding the ^{13}C nuclei. It is worth mentioning that the ^{13}C resonances of the CH ylide carbon atoms in all of our new complexes are significantly upfield compared to the 19.5 ppm observed in the reported palladium complex based on an anionic C,C,C-phosphonium ylide core pincer ligand.[11]

Compounds **2a–e** incorporate pyridine solvent as ligands due to its coordinative nature. Attempting the reaction between ligand precursor **1b** and PdCl$_2$ in less coordinative DMF solvent resulted in the formation of dimeric complex **3b**. Interestingly, the ylide carbon doublet was observed at 16.4 ppm, significantly downfield compared to all the other complexes. Similarly, the chloride anion demonstrates a coordinative effect. Using ligand precursor **1e′** with the non-coordinative BF$_4$ anion resulted in the formation of ionic complex **4e**, with two pyridine ligands coordinated around the palladium center. The ylide carbon doublet, similar to those of complexes **2**, was observed at 7.2 ppm. Yields for the two compounds are 53 and 32%, respectively. The exact structures of all the new complexes were confirmed by single-crystal X-ray diffraction studies. Notably, these complexes are air-stable and slightly soluble in common organic solvents such as CHCl$_3$ and CH$_2$Cl$_2$.

Structural descriptions

The structures of **2a–c**, **2e**, **3b**, and **4e** were successfully established by single-crystal X-ray diffraction studies (Fig. 4–6 and Fig. S1–S4 in the ESI†). In the case of **2d**, the complex converted to the dimeric complex **3d**, apparently due to the slow de-coordination of pyridine ligand during the crystal growth process. Generally, the palladium centers in complex **2** adopt a distorted square planar coordination geometry. In these complexes, the pyridine ligand is positioned *trans* to the amidate N atom, while the chloride ligand is *trans* to the coordinated C atom. The four bond angles around the palladium centers are highly distorted from the ideal 90°. This distortion is attributable to the small bite angle of the bidentate ligand. For example, in **2a**, the N1–Pd1–C8 is just 67.53(12)°. However, the summation of bond angles around the Pd center (360.2°) is very close to the ideal 360°.

The molecular structures of dimeric palladium complexes **3d** and **3b** are shown in Fig. 5 and Fig. S4,† respectively. Each dimeric palladium complex is positioned on an inversion center in these structures. The square planar coordination geometry is highly distorted, as observed in the monomeric complexes. In both structures, the Pd–Cl bond *trans* to the C atom
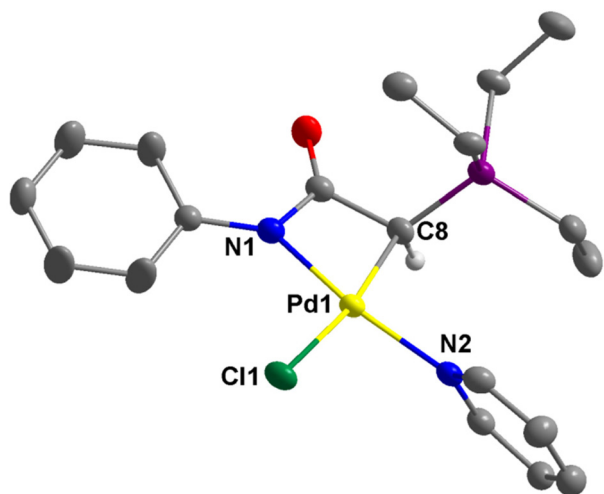
Fig. 4 Thermal ellipsoid plot of **2a** (50% probability). Hydrogen atoms except that on C8 are omitted for clarity. Selected bond distances (Å) and angles (°): Pd1–C8, 2.053(3); Pd1–Cl1, 2.3963(8); Pd1–N1, 2.023(3); Pd1–N2, 2.047(3); C8–Pd1–N1, 67.53(12); N1–Pd1–Cl1, 104.12(9); Cl1–Pd1–N2, 88.38(8); N2–Pd1–C8, 100.17(12); N1–Pd1–N2, 167.35(12); C8–Pd1–Cl1, 170.48(9).
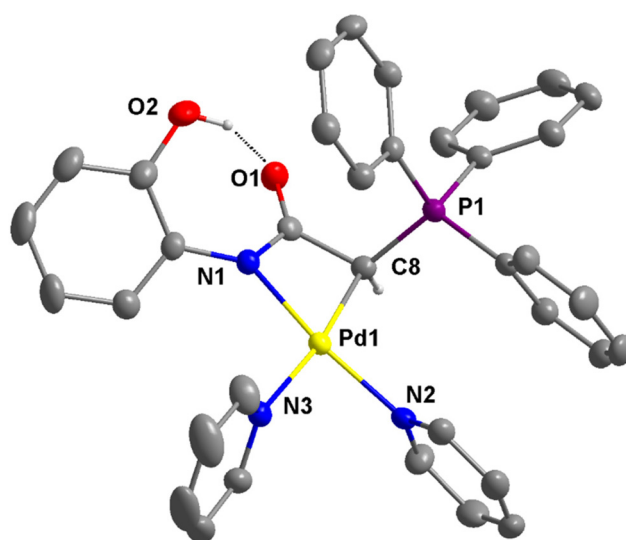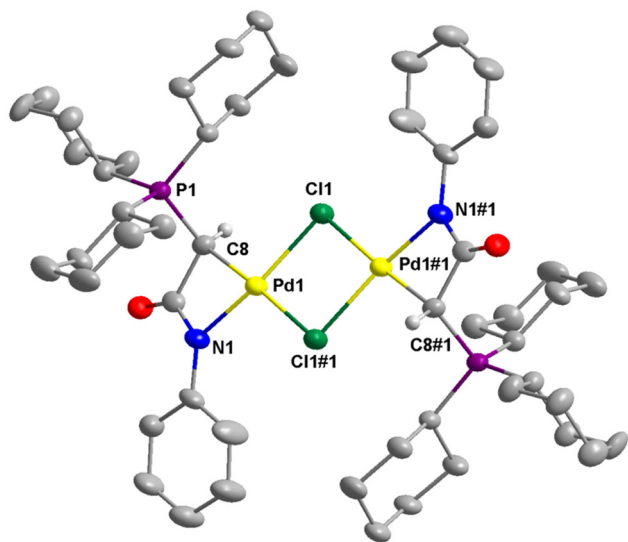

Fig. 5 Thermal ellipsoid plot of **3d** (50% probability). Hydrogen atoms except that on C8 are omitted for clarity. Selected bond distances (Å) and angles (°): Pd1–C8, 2.026(4); Pd1–N1, 2.034(4); Pd1–Cl1, 2.3491(11); Pd1–Cl1#1, 2.4167(11); Cl1#1–Pd1–N1, 108.66(11); N1–Pd1–C8, 68.07(16); C8–Pd1–Cl1, 100.38(13); Cl1–Pd1–Cl1#1, 83.94(4); N1–Pd1–Cl1, 166.95(11); Cl1#1–Pd1–C8, 176.67(13). Symmetry code #1: 1 − x, 1 − y, 1 − z.

is longer compared to that *trans* to the N atom (*e.g.*, 2.416(11) *vs.* 2.349(11) Å in **3d**), indicating a higher *trans* influence from the coordinated carbon atom. The nonbonding Pd⋯Pd distances in **3d** and **3b** are 3.571 and 3.467 Å, respectively.

The molecular structure of the cationic portion of **4e** is shown in Fig. 6. The two unequal Pd–N bond distances are the most notable structural feature. The bond distance *trans* to the

Fig. 6 Thermal ellipsoid plot of the cationic portion of **4e** (50% probability). Hydrogen atoms except that on C8 and O2 are omitted for clarity. Selected bond distances (Å) and angles (°): Pd1–C8, 2.048(3); Pd1–N1, 2.029(2); Pd1–N2, 2.043(2); Pd1–N3, 2.111(3); C8–Pd1–N1, 67.28(11); N1–Pd1–N3, 104.41(10); N2–Pd1–N3, 87.28(10); N2–Pd1–C8, 100.91(11); C8–Pd1–N3, 171.57(11); N1–Pd1–N2, 167.53(10). The intramolecular hydrogen bond is indicated by a broken line.

coordinated carbon atom is longer at 2.111(3) Å, while that *trans* to the nitrogen atom is much shorter at 2.043(2) Å. The greater *trans* influence exerted by the carbon atom compared to the nitrogen atom in the structure of **4e** is consistent with that observed in **3d** and **3b**, as well as the reported structure of [Pd{NPhC(O)CHC(O)Ph}(bipy)].[32] Similar to the structure of **2e** (see Fig. S3†), an intramolecular OH⋯O hydrogen bond is also present in **4e**. The O⋯O distances of 2.564 and 2.607 Å, respectively, are observed in these structures.

Complex **3d**, featuring the bulky PCy$_3$ moiety, exhibits the shortest Pd–C bond distance of 2.026(4) Å compared to the others, which range from 2.048 to 2.082 Å. Notably, to the best of our knowledge, the Pd–C bond in complex **3d** is the shortest among compounds containing a Pd–CHPY moiety, where Y represents a non-hydrogen atom.[3,6,11,30,32,46,47] For instance, the Pd–C bond distances are 2.070(7) and 2.0546 Å in the two reported structures of palladalactams derived from acetoacetanilides.[30,32] The sizeable *trans* influence of the coordinated carbon in **3d** results in the longest *trans* Pd–Cl bond of 2.4167(11) Å among the complexes, varying from 2.3624 to 2.3963 Å. Importantly, the installation of bulky PCy$_3$ moiety in **3d** resulted in the ligand showing the largest C–Pd–N bite angle of 68.07(16)°, while all others have smaller angles in the range of 66.99 to 67.53°. This indicates that not only the electronic effect but also the steric property of the new ligand framework can be easily modulated by selecting different phosphines. Additionally, the C–Pd–N bite angles of these phosphine-based palladalactams are larger than those of 65.4 and 66.6° in the two reported imidazole-based palladalactams (see Fig. 1).[33]

Catalytic activities

The catalytic application of the new palladium complexes in the Mizoroki–Heck coupling reaction of aryl halides with alkene was investigated. Table 1 presents the screening of the catalytic precursors. The benchmark reaction involves the coupling of 4-chloroacetophenone and styrene under our previously reported reaction conditions.[48,49] Entries 1, 2, 4, and 7 highlight that complexes **2a**, **2b**, **2d**, and the ionic complex **4e** are highly promising catalysts, delivering excellent yields of the product (>95%) under a mild 0.2 mol% Pd loading. Surprisingly, entries 3 and 6 reveal that complexes **2c** and **3b** are inactive. The Pd loading was then reduced to 0.1 mol% to differential the catalytic activities of the four complexes. Entries 8 and 10 show that complexes **2a** and **2d**, featuring electron-donating trialkylphosphine moieties, outperform complexes **2b** and **4e**, with complex **2a** slightly more active than **2d**. To further confirm the efficiency of **2a**, the Pd loading was further decreased to 0.05 mol%. Under such a low Pd loading, complex **2a**, bearing the electron-donating PEt_3 moiety, still delivers a decent 49% yield of the product, while complex **2d** shows no activity at all (entries 12 *vs.* 13).
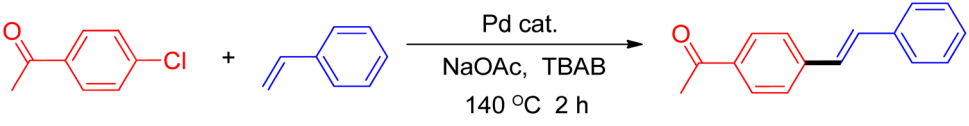
Time–yield curves of the reaction catalyzed by precatalysts **2a**, **2b**, and **2d**, as shown in Fig. S5,† clearly indicate that complex **2a** is the most efficient complex. Interestingly, there is an indication period of approximately 30 minutes in each instance, implying that the complexes are not active species. To verify this, catalytic solutions containing the complexes but without substrates in DMSO-d_6 were heated at 140 °C for 30 minutes. Subsequently, the solutions were analyzed using $^{31}P\{^1H\}$ NMR spectroscopy (Fig. S6 and S7†). In the cases of **2a** and **2d** containing trialkylphosphines, an additional small signal, approximately 1–2 ppm upfield to those of catalytic precursors, was observed. These extra peaks were tentatively identified as the active palladium(0) species $[LPd^0]^-$ resulting from the reduction of complexes **2a** and **2d**. It is worth noting that after heating the solutions, palladium black was observed for all three solutions. We hypothesize that DMSO is a less effective solvent for stabilizing the palladium(0) species. In contrast, neat TBAB at high temperatures is much better at stabilizing the species. Conversely, in the case of **2b**, no such extra species was observed by the ^{31}P NMR spectroscopy, likely due to its poorer stability in DMSO solvent than the other two complexes. Noteworthy, $[LPd^0]^-$ from **2a** possesses the strongest Pd–C and Pd–N bonds and is the most electron-donating complex according to our theoretical calculation (*vide infra*).

With the optimal catalyst precursor **2a** in hand, we embarked on refining the reaction conditions for further enhancement. Various combinations of bases and solvents were tested at different temperatures (Table 2). The initial attempts (entries 1–4) revealed that complex **2a** was inactive in an aqueous solvent containing the ionic salt tetrabutylammonium bromide (TBAB) with K_3PO_4 as the base (entry 1). Similarly, the complex showed inactivity in pure organic solvents DMF and NMP using NEt_3 and K_2CO_3 as bases at temperatures below 130 °C (entries 2–4). Entry 5 indicates the complex's activity in DMA as the solvent with 10 mol% TBAB and K_2CO_3 as the base, yielding a decent 56% product yield. Utilizing the molten salt TBAB at 140 °C as the solvent, an optimum 97% yield of coupled product was achieved using NaOAc as the base in 2 h (entry 6). However, substituting TBAB with DMA led to a significant reduction in yield (entry 7).

Following the optimization of reaction conditions, a thorough exploration of the substrate scope was undertaken
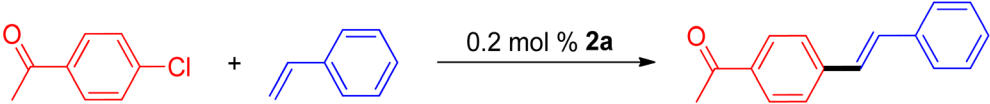

Table 1 Screening of palladium catalyst precursors for the Mizoroki–Heck coupling reaction between 4-chloroacetophenone and styrene[a]

Entry	Cat.	Pd (mol%)	Yield (%)
1	**2a**	0.2	97 (94/6)
2	**2b**	0.2	95 (95/5)
3	**2c**	0.2	0
4	**2d**	0.2	97 (94/6)
5	**2e**	0.2	88 (94/6)
6	**3b**	0.2[b]	0
7	**4e**	0.2	97 (94/6)
8	**2a**	0.1	95 (93/7)
9	**2b**	0.1	89 (94/6)
10	**2d**	0.1	91 (93/7)
11	**4e**	0.1	32 (93/7)
12	**2a**	0.05	49 (94/6)
13	**2d**	0.05	0

[a] Reaction conditions: 1.4 mmol of styrene, 1.0 mmol of aryl halide, 1.1 mmol of NaOAc, 2 g of TBAB, Pd cat., 140 °C. Yields are determined by using 1,3,5-trimethoxybenzene as the internal standard. Ratios of *anti/gem* isomers in parenthesis. [b] For dimeric complex **3b**, 0.1 mol% of the complex was used.

Table 2 Optimization of reaction conditions for Mizoroki–Heck coupling[a]

Entry	Base	Solvent	Temp. (°C)	Time (h)	Yield (%)
1[b]	K_3PO_4	$TBAB/H_2O$	110	12	0
2[c]	NEt_3	DMF	120	2	0
3[d]	K_2CO_3	DMF	80	2	0
4[e]	K_2CO_3	NMP	130	2	0
5[f]	K_2CO_3	TBAB/DMA	120	6	56 (98/2)
6[g]	NaOAc	TBAB	140	2	97 (94/6)
7[h]	NaOAc	DMA	140	2	19 (95/5)

[a] Reaction conditions: 1.0 mmol of 4-chloroacetonphenone, 1.4 mmol of styrene, 0.2 mol% **2a**. Yields determined by NMR using 1,3,5-trimethoxybenzene as the internal standard. Ratios of *anti/gem* isomers in parenthesis. [b] K_3PO_4 (1.5 mmol), TBAB (0.5 mmol), H_2O (2.0 mL). [c] NEt_3 (1.5 mmol), DMF (2.0 mL). [d] K_2CO_3 (2.0 mmol), DMF (6.0 mL). [e] K_2CO_3 (1.1 mmol), NMP (3.0 mL). [f] K_2CO_3 (1.0 mmol), TBAB (10 mol%), DMA (4.0 mL). [g] NaOAc (1.1 mmol), TBAB (2.0 g). [h] NaOAc (2.0 mmol), DMA (3.0 mL).

(Table 3). Notably, employing a reduced Pd loading of 0.1 mol% yielded comparable results to the higher 0.2 mol% loadings, promoting the preference for the former, as indicated in entries 1 *vs.* 8 of Table 1. Entries 1–13 showcase the couplings of a wide range of aryl chlorides with varying electronic properties with styrene. Generally, good to excellent yields of coupled products can be achieved with electron-deficient aryl chlorides in 2 h (entries 1–6). Compared to the *para*-substituted 4-chloroacetophenone, an extended reaction time of 12 h was required for the sterically hindered *meta*-substituted isomer (entries 3 *vs.* 7). However, the catalyst system is less efficient in utilizing electron-neutral or electron-rich aryl chlorides. Entries 8 shows that a low 36% yield of *trans*-stilbene was obtained from chlorobenzene in 12 h. Even with an increased Pd loading of 0.2 mol%, a mere 12% yield was obtained using the highly unreactive 4-chloroanisole as the substrate. For substrates featuring methoxy substituents on the phenyl rings, aryl bromides, known for their enhanced reactivity, were investigated. A significant improvement was observed, with an 84% yield of 4-methoxystilbene achieved using the bromo analog (entries 9 *vs.* 10). Additionally, a decent 61% yield was attained when 3,4,5-trimethoxyphenyl bromide was employed as the substrate. For sterically hindered *meta*- and *ortho*-methoxyphenyl bromides, reduced product yields of 54% and 28%, respectively, were obtained (entries 12 and 13). Expanding beyond styrene, the catalyst system proved highly efficient with *n*-butyl acrylate as the alkene partner (entries 14–18). For examples, quantitative yields of coupled products were achieved in 6 h when 4-chlorobenzonitrile and 4-chloroacetophenone were used (entries 14 and 15). Notably, a very good 87% yield of the coupled product was achieved with the electron-rich 4-bromoanisole as the substrate, employing an increased 0.2 mol% Pd loading (entry 19).

The catalytic performance of complex **2a** was compared with other reported palladium complexes in the literature (Table 4). The selected catalyst systems were tested for catalyzing the coupling reaction between 4-chloroacetophenone and styrene. Turnover frequencies (TOFs) were estimated from reported data to compare the catalytic efficiency among different complexes, using the mole percentage of Pd loading, the reaction yield, and the reaction time. Complex **2a** displayed the highest TOF of 475 h^{-1} among all the selected catalyst systems (entry 1). The ligand-free palladium acetate displayed the next highest TOF (395 h^{-1}) (entry 2).[50] The reported tetra-nuclear Pd aNHC complex was highly effective in utilizing electron-rich aryl chloride substrates.[48] However, it shows a lower TOF value of 248 h^{-1} compared to complex **2a** in the reaction with the electron-deficient substrate (entries 1 *vs.* 3). The reported C,C-type palladacycles also displayed a good TOF value of 235 h^{-1} (entry 4). All other catalyst systems, including Pd-NHC complexes such as PEPPSI complex $PdCl_2(IPr)(3-py)$,[49] $PdBr_2(bis-NHC)$,[51] and Pd-pyrimidine-based NHC,[52] *etc.*, displayed much inferior TOF values, all below 100 h^{-1} (entries 5–12).

Computational studies

Finally, the Wiberg bond indices (WBIs) were calculated using natural bond orbital (NBO) analysis[58] to determine the bond orders of the Pd–C and Pd–N bonds between the coordinated bidentate ligands and metal centers in compounds **2a–d** (Table 5). Due to the strong electron-donating property of the PEt_3 moiety, the Pd–C and Pd–N bonds in complex **2a** are the strongest among the four complexes. The Pd–C bond in complex **2c** is the second strongest. Furthermore, to understand the different donating abilities of the bidentate ligands, a charge decomposition analysis (CDA) was performed on $[LPd^0]^-$ (L = bidentate ligand) (see also Table 5).[59] $[LPd^0]^-$ is believed to be the active species resulted from the *in situ* reduction of the Pd(II) pre-catalyst in the catalytic cycle. The CDA results confirmed that, again, the ligand containing PEt_3 moiety in **2a** is the most electron-donating, consistent with the NMR data described above.
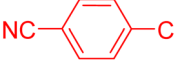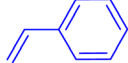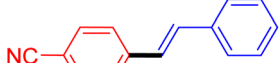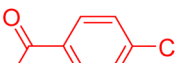
Table 3 Substrate scope[a]
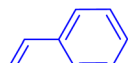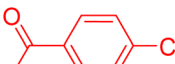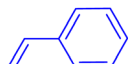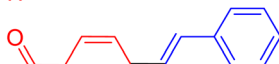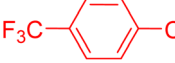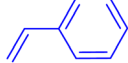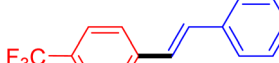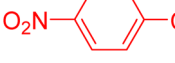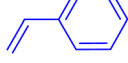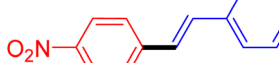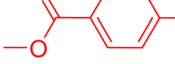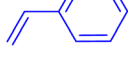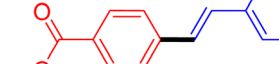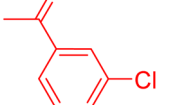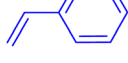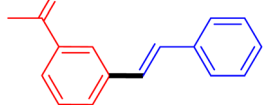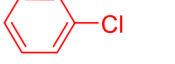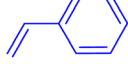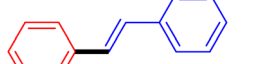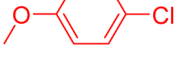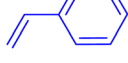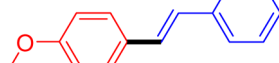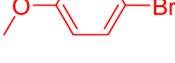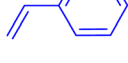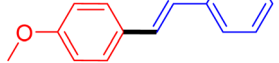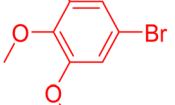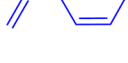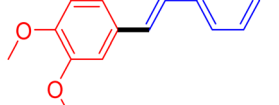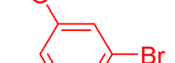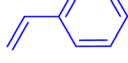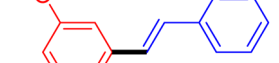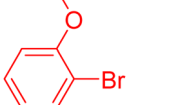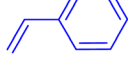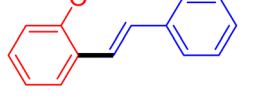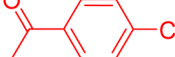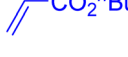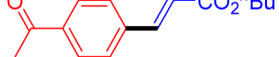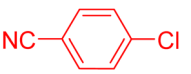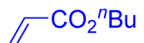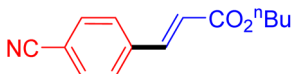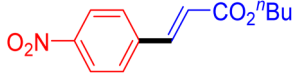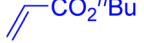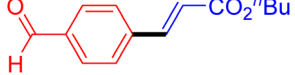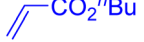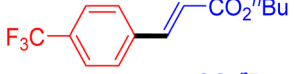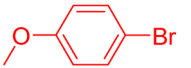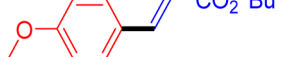
Entry	Ar–X	Alkene	Product	Time (h)	Yield (%)
1				2	99
2				2	98
3				2	94
4				2	90
5				2	78
6				2	75
7				12	43
8				12	36
9				12	12[b]
10				12	84
11				12	61
12				12	54
13				12	28[b]
14				6	99[b]

Table 3 (Contd.)

Entry	Ar–X	Alkene	Product	Time (h)	Yield (%)
15	NC–C₆H₄–Cl	$CO_2{}^nBu$	NC–C₆H₄–CH=CH–$CO_2{}^nBu$	6	99[b]
16	O_2N–C₆H₄–Cl	$CO_2{}^nBu$	O_2N–C₆H₄–CH=CH–$CO_2{}^nBu$	6	90[b]
17	OHC–C₆H₄–Cl	$CO_2{}^nBu$	OHC–C₆H₄–CH=CH–$CO_2{}^nBu$	6	77[b]
18	F_3C–C₆H₄–Cl	$CO_2{}^nBu$	F_3C–C₆H₄–CH=CH–$CO_2{}^nBu$	6	72[b]
19	MeO–C₆H₄–Br	$CO_2{}^nBu$	MeO–C₆H₄–CH=CH–$CO_2{}^nBu$	12	87[b]

[a] Reaction conditions (unless otherwise specified): 1.0 mmol aryl halide, 1.4 mmol alkene, 1.1 mmol NaOAc, 2 g of TBAB, 0.1 mol% **2a**, 140 °C, 2–12 h. Isolated yield. [b] 0.2 mol% **2a**.

Table 4 Comparison of catalytic activities between complex **2a** and other palladium complexes in the Mizoroki–Heck coupling reaction of 4-chloroacetophenone and styrene

Entry	Complex type	Mol% Pd	Time (h)	Yield (%)	TOF (h^{-1})	Ref.
1	Palladalactam **2a**	0.1	2	95[a]	475	This work
2	Ligand-free Pd(OAc)₂	0.1	2	79[a]	395	50
3	Tetranuclear Pd aNHC	0.2	2	99[a]	248	48
4	C,C-type palladacycles	0.2	2	94[a]	235	50
5	Oxime-based palladacycle	0.5	2	100[b]	100	53
6	PdCl₂/amino-chroman-4-one	0.3	3.5	87[c]	83	54
7	PdCl₂(IPr)(3-py)	0.2	2	26[a]	65	49
8	PdBr₂(bis-NHC)	0.01	30	—	38	51
9	Benzothiazole-oxime PdCl₂	0.5	10	87[b]	17	55
10	PEPPSI-type Pd-NHC	1	15	>99[b]	6.6	56
11	Pd-pyrimidine-based NHC	1	20	88[b]	4.4	52
12	[Pd₂(Xantphos)₂(4,4′-SC₁₂H₈S)]₂(OTf)₄	2	24	15[a]	0.3	57

[a] NMR yield. [b] GC yield. [c] Isolated yield.

Table 5 WBI and CDA analyses[a]

Complexes	WBI (Pd–C)	WBI (Pd–N)	[LPd⁰]⁻	d[b]	b[c]	r[d]	$(d + b)$	$b/(d + b)$
2a	0.6269	0.4375	[LᵃPd⁰]⁻	0.192374	0.121512	−0.138286	0.313886	38.7%
2b	0.6169	0.4330	[LᵇPd⁰]⁻	0.181107	0.142346	−0.176867	0.323453	44.0%
2c	0.6214	0.4319	[LᶜPd⁰]⁻	0.180921	0.140253	−0.176829	0.321174	43.7%
2d	0.6168	0.4271	[LᵈPd⁰]⁻	0.178887	0.131640	−0.151839	0.310527	42.4%

[a] At the M06-L/def2TZVP level. [b] Number of electrons donated from the ligand to the Pd atom. [c] Number of electrons donated from the Pd atom to the ligand. [d] Closed-shell interaction.

Conclusion

A new series of ligand precursors has been successfully developed to prepare palladalactams. These precursors, synthesized *via* a simple one-step reaction between 2-chloro-*N*-phenylacetamide and various monophosphines, offer a versatile platform for tailoring the electronic and steric properties of ligand frameworks. Additionally, their exceptional stability in ambient air enhances their practical applicability. The successful synthesis of a new palladalactam, incorporating an electron-donating triethylphosphine moiety, underscores the catalytic potential of these ligand systems, particularly in the Mizoroki–Heck coupling reaction. Theoretical calculations further support the superior electron-donating ability of this ligand, highlighting its role in forming robust Pd–C bonds. Our ongoing efforts in fine-tuning the ligand framework aim to optimize catalytic performance across a range of Pd-catalyzed reactions. This research sets the stage for the continued exploration and application of tailored ligand systems based on phosphonium ylides in homogeneous catalysis.

Conflicts of interest

There are no conflicts of interest to declare.

Acknowledgements

References

1 H. Schmidbaur, *Angew. Chem., Int. Ed. Engl.*, 1983, **22**, 907–927.
2 J. Vicente, M.-T. Chicote, I. Saura-Llamas, M.-J. López-Muñoz and P. G. Jones, *J. Chem. Soc., Dalton Trans.*, 1990, 3683–3689, DOI: 10.1039/DT9900003683.
3 L. R. Falvello, S. Fernández, R. Navarro, A. Rueda and E. P. Urriolabeitia, *Inorg. Chem.*, 1998, **37**, 6007–6013.
4 L. R. Falvello, S. Fernández, R. Navarro, A. Rueda and E. P. Urriolabeitia, *Organometallics*, 1998, **17**, 5887–5900.
5 A. Spannenberg, W. Baumann and U. Rosenthal, *Organometallics*, 2000, **19**, 3991–3993.
6 R. Zurawinski, B. Donnadieu, M. Mikolajczyk and R. Chauvin, *J. Organomet. Chem.*, 2004, **689**, 380–386.
7 L. R. Falvello, J. C. Ginés, J. J. Carbó, A. Lledós, R. Navarro, T. Soler and E. P. Urriolabeitia, *Inorg. Chem.*, 2006, **45**, 6803–6815.
8 S. J. Sabounchei, M. Hosseinzadeh, S. Salehzadeh, F. Maleki and R. W. Gable, *Inorg. Chem. Front.*, 2017, **4**, 2107–2118.
9 E. Serrano, R. Navarro, T. Soler, J. J. Carbó, A. Lledós and E. P. Urriolabeitia, *Inorg. Chem.*, 2009, **48**, 6823–6834.
10 R. Taakili, C. Lepetit, C. Duhayon, D. A. Valyaev, N. Lugan and Y. Canac, *Dalton Trans.*, 2019, **48**, 1709–1721.
11 R. Taakili, C. Barthes, C. Lepetit, C. Duhayon, D. A. Valyaev and Y. Canac, *Inorg. Chem.*, 2021, **60**, 12116–12128.
12 D. A. Valyaev and Y. Canac, *Dalton Trans.*, 2021, **50**, 16434–16442.
13 D. A. Petrone, K. M. Szkop, L. Miao, P. St. Onge, Z.-W. Qu, S. Grimme and D. W. Stephan, *Angew. Chem., Int. Ed.*, 2021, **60**, 18547–18551.
14 Y. Shi, B.-W. Pan, J.-S. Yu, Y. Zhou and J. Zhou, *ChemCatChem*, 2021, **13**, 129–139.
15 M. El Kadiri, A. Chihab, R. Taakili, C. Duhayon, D. A. Valyaev and Y. Canac, *Organometallics*, 2022, **41**, 456–466.
16 M. Ameskal, R. Taakili, E. S. Gulyaeva, C. Duhayon, J. Willot, N. Lugan, C. Lepetit, D. A. Valyaev and Y. Canac, *Inorg. Chem.*, 2023, **62**, 20129–20141.
17 T. Scherpf, C. Schwarz, L. T. Scharf, J.-A. Zur, A. Helbig and V. H. Gessner, *Angew. Chem., Int. Ed.*, 2018, **57**, 12859–12864.
18 P. Weber, T. Scherpf, I. Rodstein, D. Lichte, L. T. Scharf, L. J. Gooßen and V. H. Gessner, *Angew. Chem., Int. Ed.*, 2019, **58**, 3203–3207.
19 X.-Q. Hu, D. Lichte, I. Rodstein, P. Weber, A.-K. Seitz, T. Scherpf, V. H. Gessner and L. J. Gooßen, *Org. Lett.*, 2019, **21**, 7558–7562.
20 J. Tappen, I. Rodstein, K. McGuire, A. Großjohann, J. Löffler, T. Scherpf and V. H. Gessner, *Chem. – Eur. J.*, 2020, **26**, 4281–4288.
21 A. Sarbajna, V. S. V. S. N. Swamy and V. H. Gessner, *Chem. Sci.*, 2021, **12**, 2016–2024.
22 S. Lapointe, A. Sarbajna and V. H. Gessner, *Acc. Chem. Res.*, 2022, **55**, 770–782.
23 W. A. Herrmann, K. Öfele, D. von Preysing and S. K. Schneider, *J. Organomet. Chem.*, 2003, **687**, 229–248.
24 E. A. B. Kantchev, C. J. O'Brien and M. G. Organ, *Angew. Chem., Int. Ed.*, 2007, **46**, 2768–2813.
25 N. Marion and S. P. Nolan, *Acc. Chem. Res.*, 2008, **41**, 1440–1449.
26 S. Díez-González, N. Marion and S. P. Nolan, *Chem. Rev.*, 2009, **109**, 3612–3676.
27 G. C. Fortman and S. P. Nolan, *Chem. Soc. Rev.*, 2011, **40**, 5151–5169.
28 C. Valente, S. Çalimsiz, K. H. Hoi, D. Mallik, M. Sayah and M. G. Organ, *Angew. Chem., Int. Ed.*, 2012, **51**, 3314–3332.
29 M. N. Hopkinson, C. Richter, M. Schedler and F. Glorius, *Nature*, 2014, **510**, 485–496.
30 W. Henderson, J. Fawcett, R. D. W. Kemmitt, C. Proctor and D. R. Russell, *J. Chem. Soc., Dalton Trans.*, 1994, 3085–3090, DOI: 10.1039/DT9940003085.
31 W. Henderson, B. K. Nicholson and A. G. Oliver, *Polyhedron*, 1994, **13**, 3099–3104.
32 W. Henderson, A. G. Oliver, C. E. F. Rickard and L. J. Baker, *Inorg. Chim. Acta*, 1999, **292**, 260–265.
33 J.-Y. Lee, Y.-H. Huang, S.-Y. Liu, S.-C. Cheng, Y.-M. Jhou, J.-H. Lii and H. M. Lee, *Chem. Commun.*, 2012, **48**, 5632–5634.
34 S.-J. Chen, Y.-D. Lin, Y.-H. Chiang and H. M. Lee, *Eur. J. Inorg. Chem.*, 2014, 1492–1501.

35 M. Oestreich, *The Mizoroki–Heck Reaction*, John Wiley & Sons, Ltd, 2009.

36 K. R. Balinge and P. R. Bhagat, *C. R. Chim.*, 2017, **20**, 773–804.

37 P. J. Anju, M. Neetha and G. Anilkumar, *ChemistrySelect*, 2022, **7**, e202103564.

38 T. Mino, Y. Shirae, Y. Sasai, M. Sakamoto and T. Fujita, *J. Org. Chem.*, 2006, **71**, 6834–6839.

39 G.-R. Peh, E. A. B. Kantchev, C. Zhang and J. Y. Ying, *Org. Biomol. Chem.*, 2009, **7**, 2110–2119.

40 S. Inomata, H. Hiroki, T. Terashima, K. Ogata and S.-i. Fukuzawa, *Tetrahedron*, 2011, **67**, 7263–7267.

41 A. V. Astakhov, O. V. Khazipov, A. Y. Chernenko, D. V. Pasyukov, A. S. Kashin, E. G. Gordeev, V. N. Khrustalev, V. M. Chernyshev and V. P. Ananikov, *Organometallics*, 2017, **36**, 1981–1992.

42 D. Borah, B. Saha, B. Sarma and P. Das, *J. Chem. Sci.*, 2020, **132**, 51.

43 S. Chakrabortty, M. Kaur, M. Adhikari, K. K. Manar and S. Singh, *Inorg. Chem.*, 2021, **60**, 6209–6217.

44 O. Bysewski, A. Winter and U. S. Schubert, *Inorganics*, 2023, **11**, 164.

45 R. O. Pankov, D. O. Prima, A. Y. Kostyukovich, M. E. Minyaev and V. P. Ananikov, *Dalton Trans.*, 2023, **52**, 4122–4135.

46 S. Stallinger, C. Reitsamer, W. Schuh, H. Kopacka, K. Wurst and P. Peringer, *Chem. Commun.*, 2007, 510–512, DOI: **10.1039/B609723E**.

47 B. S. Aweke, C.-H. Yu, M. Zhi, W.-C. Chen, G. P. A. Yap, L. Zhao and T.-G. Ong, *Angew. Chem., Int. Ed.*, 2022, **61**, e202201884.

48 J.-Y. Lee, Y.-S. Su, Y.-S. Wang and H. M. Lee, *Adv. Synth. Catal.*, 2019, **361**, 4714–4726.

49 C.-H. Hung, W.-Y. Zheng and H. M. Lee, *Organometallics*, 2021, **40**, 702–713.

50 C. H. Lo and H. M. Lee, *Organometallics*, 2018, **37**, 1150–1159.

51 M. A. Taige, A. Zeller, S. Ahrens, S. Goutal, E. Herdtweck and T. Strassner, *J. Organomet. Chem.*, 2007, **692**, 1519–1529.

52 J. Ye, W. Chen and D. Wang, *Dalton Trans.*, 2008, 4015–4022, DOI: **10.1039/B801264D**.

53 D. A. Alonso, C. Nájera and M. C. Pacheco, *Adv. Synth. Catal.*, 2002, **344**, 172–183.

54 D. Khan and I. Parveen, *Eur. J. Org. Chem.*, 2021, 4946–4957.

55 K. M. Dawood, *Tetrahedron*, 2007, **63**, 9642–9651.

56 Y.-C. Lin, H.-H. Hsueh, S. Kanne, L.-K. Chang, F.-C. Liu, I. J. B. Lin, G.-H. Lee and S.-M. Peng, *Organometallics*, 2013, **32**, 3859–3869.

57 P. A. Mane, S. Neogy and S. Dey, *Appl. Organomet. Chem.*, 2020, **34**, e5405.

58 E. D. Glendening, A. E. Reed, J. E. Carpenter and F. Weinhold, *NBO Version 3.1*, 2001.

59 S. Dapprich and G. Frenking, *J. Phys. Chem.*, 1995, **99**, 9352–9362.